# Subtropical cells and meridional overturning circulation pathways in the tropical Atlantic

Wilco Hazeleger[1] and Sybren Drijfhout[1]

[1]  Pathways of subtropical cells (STCs) and the basin-wide meridional overturning circulation (MOC) are studied in the tropical Atlantic using a particle tracking algorithm and transports from a high-resolution ocean model. Here 16 Sv (=$10^6$ m$^3$ s$^{-1}$) of MOC water flows to the equator from the south, primarily in the North Brazil Current. The MOC water recirculates in the tropics and, after crossing the equator about half of it, stays along the western boundary and the other half loops in a cyclonic circulation northward to join the North Equatorial Current. The STC on the Southern Hemisphere has a strength of 4 Sv. The northern STC has a strength of 1.5 Sv; it is confined to the retroflection area close to the equator and it contains primarily MOC water. In total, 5.5 Sv of MOC water entrains into the mixed layer in the tropical Atlantic. Here 2 Sv of MOC water recirculates in the southern STC and 1.5 Sv in the northern STC. The STCs are weaker than suggested from observations, but the interior flows in the model compare well to observations. The heat transport divergence that is associated with warming of MOC water masses between 10°S and 10°N is 0.22 PW (=$10^{15}$W). The fresh water transport divergence of MOC water masses in the tropical Atlantic is 0.16 Sv. It is concluded that the MOC can substantially affect the tropical circulation, but the tropical circulation itself can also affect MOC properties.

## 1.  Introduction

[2]  Heat is transferred northward in the entire Atlantic Ocean. This can be attributed to the presence of a basin-wide meridional overturning circulation (MOC) that consists of a northward branch in the upper layers, sinking at high latitudes associated with the formation of North Atlantic Deep Water and a southward return flow at depth [*Schmitz*, 1995]. In addition to this basin-wide MOC, heat and mass are transferred by shallow wind-driven overturning cells at low latitudes. In these subtropical cells (STCs), water masses subduct from the surface in the subtropics and transfer water masses subsurface to the equator where Ekman divergence drives upwelling and poleward surface flow [*McCreary and Lu*, 1994]. Western boundary currents, mesoscale eddies, and a complex structure of zonal currents near the equator complicate this circulation scheme in the tropical Atlantic [e.g., *Johns et al.*, 1990; *Schott et al.*, 1998].

[3]  In the subtropical South Atlantic, water masses are transferred equatorward below the mixed layer by both the STC and the MOC. There seems to be an unopposed subsurface flow toward the equator originating from subduction zones along the South Equatorial Current and a compensating southward surface flow [e.g., *Schott et al.*, 1998; *Fratantoni et al.*, 2000; *Hazeleger et al.*, 2003]. In the North Atlantic the MOC and the STC transfer water northward in the surface layer, while the STC transfers water southward below the mixed layer. Owing to strong interhemispheric transport by the MOC, observations and model results indicate that the zonal mean circulation north of the equator is northward in the upper ocean [e.g., *Jochum and Malanotte-Rizzoli*, 2001]. The MOC is presumably localized in the northward flowing North Brazil Current, in the along-shore currents along Guiana, and in North Brazil Current eddies. A northern STC may hardly exist because the North Equatorial Counter Current and the upwelling below the Intertropical Convergence zone can effectively block an oceanic connection between the Northern Hemisphere subtropics and the equator [*Zhang et al.*, 2003].

[4]  The ventilation of the equatorial thermocline is of importance because low-frequency tropical Atlantic climate variability is partly related to thermocline properties which are set by subduction [*Zebiak*, 1993]. Also, the properties of the MOC can be modified due to mixing and surface fluxes in the Atlantic basin. This makes the Atlantic, and the tropics in particular, an active conduit for the upper branch of the MOC. The STCs and the MOC are likely to interact with each other, but it is largely unknown to what extent.

[5]  It is our goal to determine the MOC and STC pathways and their interaction in the tropical Atlantic region. It is nearly impossible to determine these characteristics from

---

[1]Oceanographic Research, Royal Netherlands Meteorological Institute (KNMI), de Bilt, Netherlands.

observational data. Water mass analysis, tracer analysis, geostrophic, and direct current measurements can be used to determine sources of water masses [*Zhang et al.*, 2003; *Johns et al.*, 2003], but if the MOC recirculates in the STCs and ventilates multiple times in the Atlantic, its characteristics will be lost. However, we can quantify and visualize this using model results. Here we will analyze output from a high-resolution ocean model and decompose the circulation into a part that is associated with the STCs and a part that is associated with the MOC. We use seasonally averaged transports and a particle tracking algorithm. The advantage of using the Lagrangian tracking technique is that pathways of the MOC and STC can be disentangled and that the degree of recirculation can be quantified. *Blanke et al.* [1999], *Malanotte-Rizzoli et al.* [2000], and *Halliwell et al.* [2003] also used Lagrangian analysis in an ocean model to determine STC and MOC pathways. These studies used coarse resolution models and some of them used annual mean data unlike our study. In earlier studies we showed that high-frequency variability matters for the subduction sites and pathways for ventilated water [*Hazeleger et al.*, 2003; *Hazeleger and de Vries*, 2003b]. Here we build further upon our analysis of the ventilation of the equatorial thermocline in the Atlantic.

## 2. Methods

### 2.1. Model

[6] Data from the high-resolution global ocean model OCCAM [*Webb et al.*, 1997] are used in this study. This primitive equation model has realistic topography, a horizontal resolution of 0.25°, and 36 vertical levels with variable thickness. A Laplacian horizontal diffusion and friction is used. The diffusion coefficient is 100 m$^2$ s$^{-1}$ and the viscosity is 200 m$^2$ s$^{-1}$. The vertical mixing of tracers is parameterized according to the *Pacanowski and Philander* [1981] scheme. This results in diffusivities on the order of 0.5 cm$^2$ s$^{-1}$ away from regions with strong shears.

[7] The surface forcing consists of a relaxation of sea surface temperature to data from *Reynolds and Smith* [1994] and sea surface salinity to data of *Levitus et al.* [1994]. The model has been initialized using temperature and salinity data from *Levitus and Boyer* [1994] and *Levitus et al.* [1994]. The model has been spun up for 9 years using monthly mean winds and wind stresses from the European Centre for Medium-Range Weather Forecasts [*Gibson et al.*, 1997]. In the following 3 years, six hourly winds were used used.

[8] Different aspects of the simulated circulation relevant to the problem that is studied here are presented by *Hazeleger et al.* [2003], *Hazeleger and de Vries* [2003], *Drijfhout et al.* [2003], and *Donners et al.* [2005]. We refer the reader to these studies for general characteristics on South Atlantic and tropical Atlantic circulation simulated by the model.

### 2.2. Analysis Tools

[9] To determine the pathways of the MOC and STCs, we use a particle tracking algorithm that is described by *Döös* [1995] and *Blanke and Raynaud* [1997]. This algorithm has been modified to allow for time-dependent fields by *de Vries and Döös* [2001]. Seasonally averaged mass fluxes are

used to trace water masses off-line. We include eddy-induced mass fluxes obtained from 5-day running mean data as described by *Hazeleger et al.* [2003]. By including eddy-induced fluxes, the time-mean effect of eddies on the circulation is resolved and spurious diapycnic mass fluxes are reduced. High-frequency variability also acts to disperse trajectories, but as shown by *Goodman et al.* [2005], most dispersion is due to seasonal variability and less due to higher-frequency variability. To retain a correct amplitude of the seasonal cycle, all seasonally varying fields were interpolated according to the method of *Killworth* [1996].

[10] The particles are seeded uniformly in space over the face of each grid box that meets a chosen starting criterion [*Blanke and Raynaud*, 1997]. The number of particles is proportional to the transport across the face of the grid box. In this way they are grouped in regions where the transport is highest. Also, the release of particles is distributed over time. In this study each particle represents 0.001 Sv (Sv = $10^6$ m$^3$ s$^{-1}$). The particles are traced using the transport at each gridpoint while obeying mass conservation for each particle along its trajectory. The method is flexible and allows for forward and backward tracing between predefined sections or planes.

[11] Except for analyzing individual trajectories we also determine Lagrangian stream functions according to *Blanke et al.* [1999]. Each particle is associated with a transport that is recorded and summed on each gridpoint. This results in a three-dimensional nondivergent field that can be integrated to derive a transport stream function. This approach allows for concise description of the transport by the ensemble of particles that is much easier to interpret than the pathways of individual trajectories.

## 3. Results

### 3.1. Decomposition of MOC and STC Transports

[12] Since both the upper branch of the MOC and the STCs are found in the upper layers of the tropical Atlantic, it is likely that the MOC and STC strongly interact. Therefore we will show the flow associated with the STCs and the MOC separately. The STC will be defined by water that is expelled poleward in the mixed layer near the equator and returns to the equator below the mixed layer after being subducted. The upper limb of the MOC constitutes of water masses that enter the basin in the south at 30°S and leave the tropical Atlantic region in the north at 20°N.

### 3.1.1. Pathways

[13] To determine the structure of the STC in the Southern Hemisphere, we released particles at 2°S below the mixed layer (defined as the depth at which the density is 0.1 kg m$^{-3}$ greater than its surface value), traced them backward in time, and stopped tracking after they return to 2°S above the mixed layer. This is done in a similar fashion for the northern STC. This captures the poleward flow in the mixed layer, subduction, and then equatorward flow below the mixed layer. The Lagrangian stream function of the STC is shown in Figure 1. As described in the previous section, this stream function describes the pathways of an ensemble of trajectories. It is a subset of all possible trajectories in the tropical Atlantic. The STC in the Southern Hemisphere is rather weak. South of 10°S it transfers only 1 Sv. Closer to the equator the STC strengthens up to 4 Sv. After subduc-
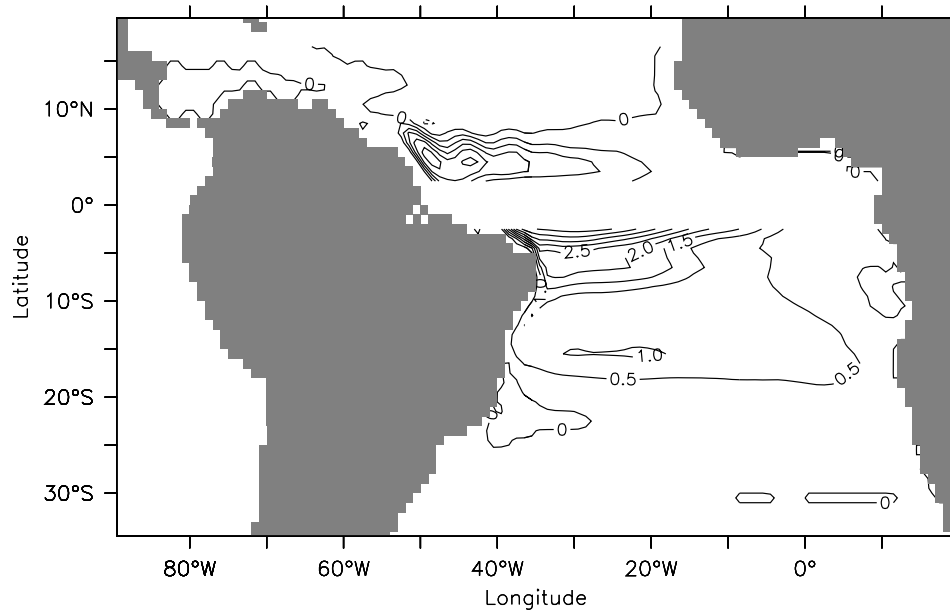
**Figure 1.** Stream function (in Sv) of particles that start at 2°S below the mixed layer and are traced backward until they return at 2°S in the mixed layer without leaving the Atlantic basin (bottom). Same for 2°N (top). These particles represent the STC in both hemispheres. Contour interval = 0.5 Sv.

tion most water follows the western boundary toward the equator in accordance with the results of *Hazeleger et al.* [2003] and *Hazeleger and de Vries* [2003]. However, close to the equator interior pathways are found as well.

[14] In the Northern Hemisphere the STC is primarily located in the retroflection region and in the region of the North Equatorial Counter Current. This is in accordance with the notion that there is no strong STC in the Northern Hemisphere, partly due to the presence of the MOC and partly due to the potential vorticity ridge generated by the

winds associated with Intertropical Convergence Zone and the North Equatorial Counter Current [*Zhang et al.*, 2003]. This implies that Salinity Maximum Water which is found in the subsurface layers of the subtropical North Atlantic cannot reach the equator through a northern Subtropical Cell.

[15] The pathways of the upper limb of the MOC in the Southern Hemisphere are determined by releasing particles at 2°S and trace them backward until they leave the basin at 30°S (Figure 2). As in the work of *Donners et al.* [2005]
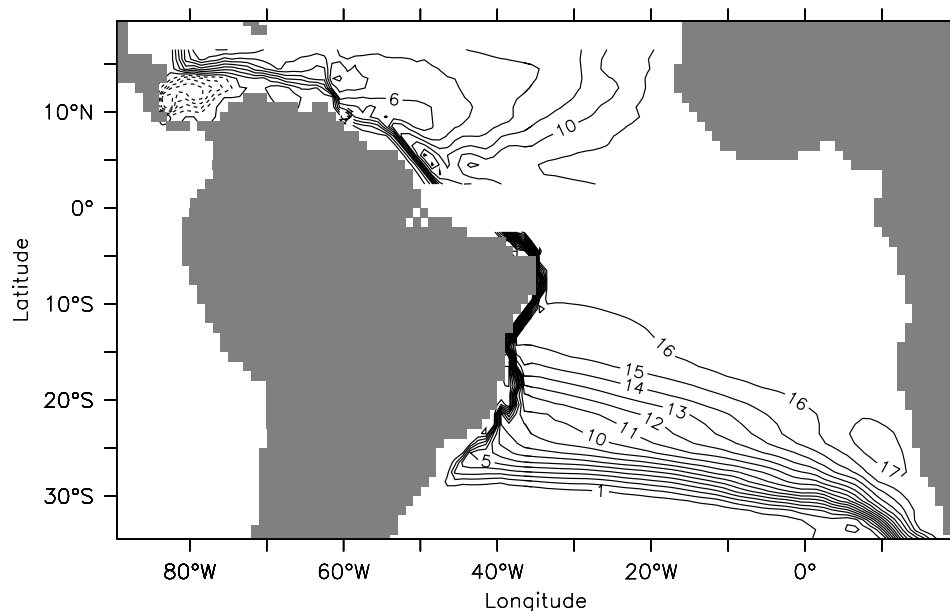


**Figure 2.** Stream function (in Sv) of particles that start at 2°S and are traced backward until they leave the basin at 30°S (bottom) and particles that start at 2°N and are traced forward until they leave the basin at 20°N (top). This represents the upper limb of the MOC in both hemispheres. Contour interval = 1 Sv.
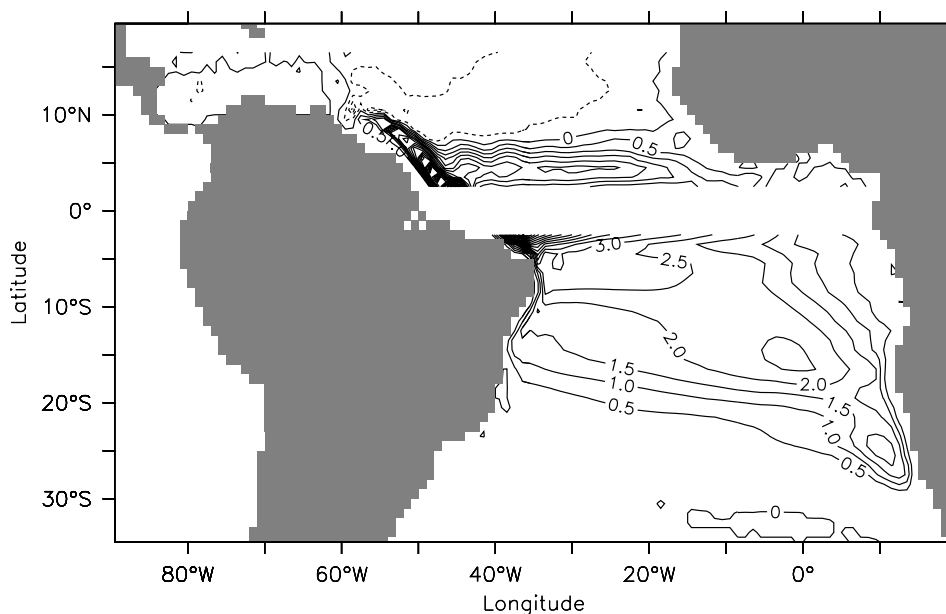
**Figure 3.** Stream function of particles (in Sv) that start at 2°S either below or in the mixed layer and are traced backward until they return at 2°S either below or in the mixed layer without leaving the Atlantic basin (bottom). These particles have not passed through the mixed layer base. Same for 2°N (top). These particles represent a horizontal, recirculating gyre flow in both hemispheres. Contour interval = 0.5 Sv.

and *Drijfhout et al.* [2003], most MOC water originates from interbasin exchange with the Indian Ocean. The upper limb of the MOC follows the South Equatorial Current and bifurcates at the western boundary to follow the North Brazil Current northward. The northward flow at the western boundary coincides with the pathway of the STC. These Lagrangian stream functions show vertically integrated transports and we discuss how much the STCs and MOC are intertwined in the vertical in the next sections.

[16] For the Northern Hemisphere, particles are traced forward from 2°N until they pass 20°N. A substantial amount of MOC water retroflects in the retroflection of the North Brazil current just north of the equator. About 5 Sv of MOC water follows the western boundary northward, probably by North Brazil Current eddies (which are present in this model and represented in the eddy-induced transports). Another 6 Sv makes an eastward excursion to follow an interior pathway. In the cyclonic circulation between 50°W and 15°W it turns northward. Some of that water upwells and moves northward in the Ekman layer. The water masses that follow this interior route ultimately join the North Equatorial Current that carries the water westward to the western boundary. Here 11.5 Sv of MOC water crosses 20°N while 16 Sv enters the basin at 30°S. The difference is due to drift in the model. Adjustment of the model circulation to the applied surface fluxes leads to a reduction of production of North Atlantic Deep Water. This leads to an apparent downwelling of Intermediate Water in the Northern Hemisphere tropical latitudes where it becomes entrained in the southward flow of North Atlantic Deep Water. However, pathways in the tropics are not strongly affected by the drift.

[17] Finally, there is a substantial amount of water that feeds the tropics that does not subduct or upwell and that is not part of the MOC. This water recirculates in horizontal

gyres either in the mixed layer or below the mixed layer. Figure 3 shows the stream function of these water masses. Again, the western boundary stands out in the south and the retroflection area in the north. Unlike the STC pathways the recirculated water extends further to the south and to the east.

### 3.1.2. Cross Sections

[18] Cross sections of the water mass pathways that were described above can reveal how much the STCs and MOC interact. In Figure 4 we show the location of particles in the STC and MOC that cross 10°S. The particles were released at 2°S and traced backward as described before. Positions are shown of particles that arrive here for the first time after being released. This cross section shows that the MOC and STC are well separated upon first approach toward the equator. Both the MOC and STC are transferring water masses northward below the mixed layer at the western boundary, but MOC water masses are located at larger depth than the STC water masses. There is a substantial interior transport of the STC as well. As we traced particles backward from 2°S, MOC water did not have a chance yet to upwell at the equator or further north and recirculate in the STC.

[19] Figure 5 shows the last time when water mass particles cross 10°S when tracing back from 2°S. For the MOC this results in the same picture as Figure 4. That is, MOC water masses transfer northward only and hardly recirculate between 10°S and 2°S. For the STC we recognize the upper limb in the mixed layer. This southward component of the flow only occurs in the interior, which indicates that the northward flowing western boundary currents are strong enough to overcome the southward Ekman transport.

[20] A similar analysis for the Northern Hemisphere shows a much different structure. When particles are re-
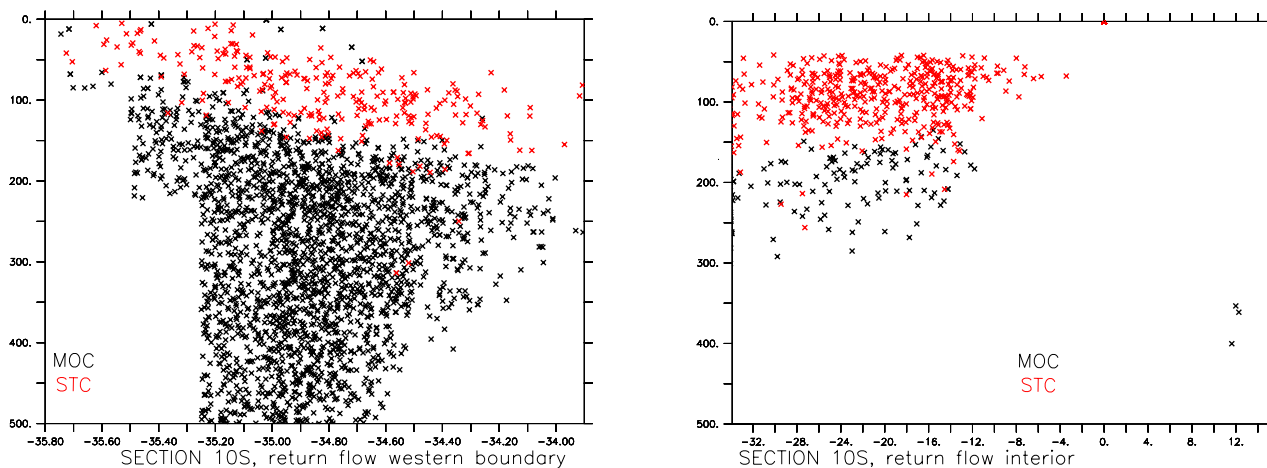
**Figure 4.** Cross section at 10°S of particles that were released at 2°S and traced backward until 10°S. This is the position where the particles pass 10°S northward for the first time (southward in a backward direction). STC and MOC particles are distinguished, that is, MOC particles leave the Atlantic basin and STC particles, when traced backward, return to 2°S above the mixed layer. Every 20th particle is shown.

leased at 2°N and traced forward, it appears that MOC water masses are partly upwelled. This results in northward transfer of both STC and MOC water masses in the mixed layer at 6°N (Figure 6). Between about 300 and 900 m depth, Antarctic Intermediate Water is transferred northward by the MOC. The transport occurs partially along the western boundary and partially in the interior in accordance with the stream function shown in Figure 2.

[21] Between the mixed layer base and 300 m there is strong recirculation near the western boundary, but in the interior the net transport is southward as indicated by the positions of the particles that cross 6°N for the last time before returning to the equator or leaving the region at 20°N (Figure 7). The MOC positions hardly change between the first time and the last time that MOC particles pass 6°N. However, the lower limb of the STC on the Northern Hemisphere is visible now in the interior at 100 m depth. So, on the Northern Hemisphere the upper branch of the

MOC and the STC interact in the mixed layer, while the return flow of the STC, which is in itself weak, is well separated from the MOC in the interior.

[22] The cross sections shown so far could not reveal the strength of interaction between the MOC and STC in the Southern Hemisphere. However, interaction takes place when we consider the location of the particles when tracing forward from 20°S up to 20°N and plot the location when particles for the last time pass 6°S. Unlike the analysis of the cross sections on the Southern Hemisphere shown before, now the parcels could upwell near the equator and recirculate. When we compare these locations with the positions of the particles that were traced backward from 2°S as in Figure 4, we see that some MOC water and STC water is found at the same locations (Figure 8). This is most notable between the surface and 150 m depth at the western boundary where the flow is northward and at 100 m depth in the interior where the meridional flow is southward. This
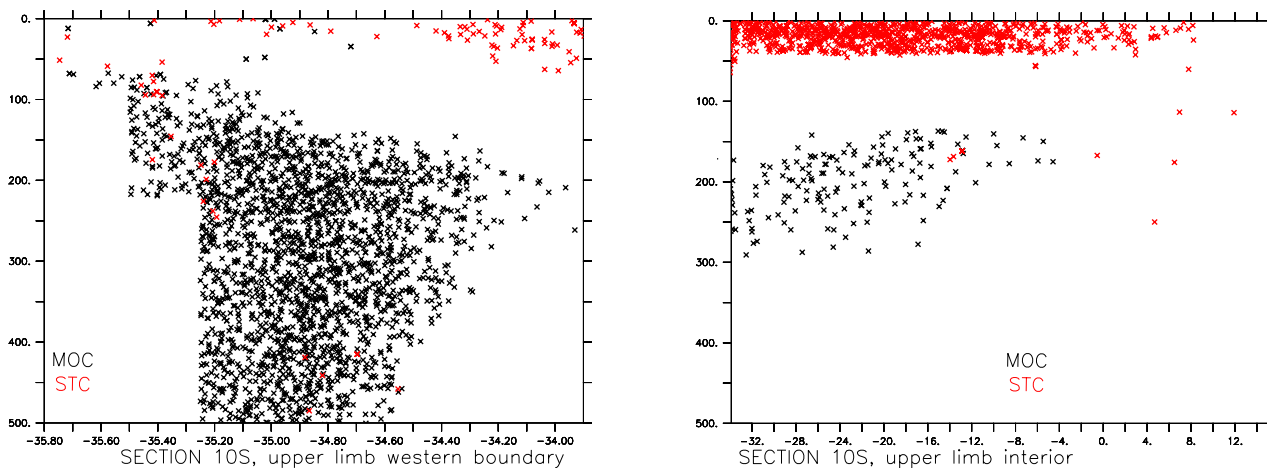


**Figure 5.** Cross section at 10°S of particles that were released at 2°S and traced backward until 10°S. This is the position where the particles pass 10°S for the last time. STC and MOC particles are distinguished, that is, MOC particles leave the Atlantic basin and STC particles, when traced backward, return to 2°S above the mixed layer. Every 20th particle is shown.
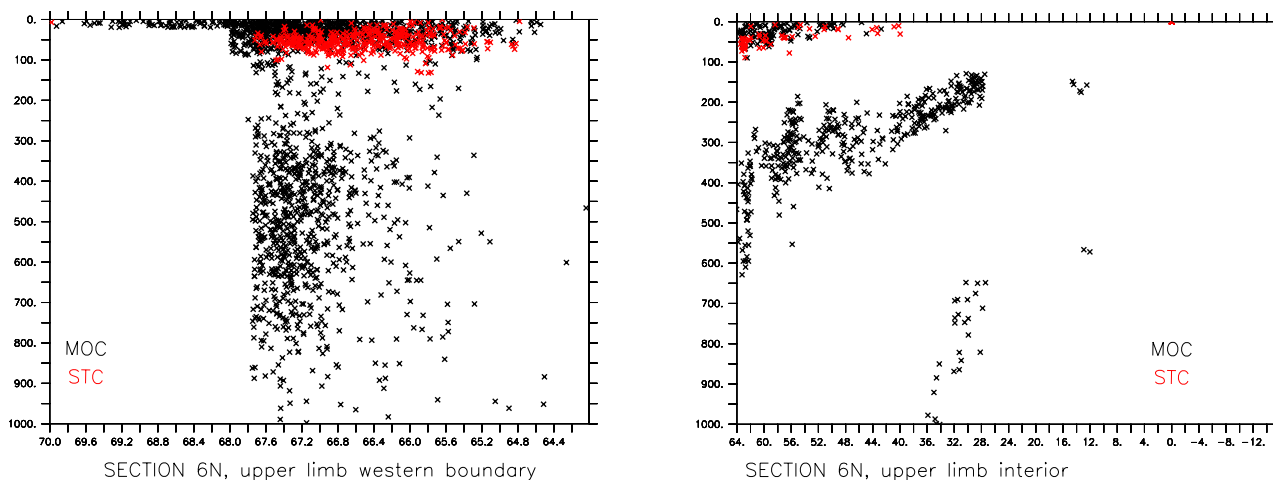
**Figure 6.** Cross section at 6°N of particles that were released at 2°N and traced forward until 6°N. This is the position where the particles pass 6°N for the first time. STC and MOC particles are distinguished, that is, MOC particles transfer northward at 20°N in the Atlantic basin and STC particles, when traced forward, return to 2°N below the mixed layer. Every 20th particle is shown.

implies that at least part of the MOC upwells in the equatorial region and recirculates in the southern STC. This is an important point as some MOC water will transform in the tropical region (see section 4).

[23] Figure 6 and Figure 8 indicate MOC-STC interaction. To quantify the interaction, we tracked the origins of STC water and determined whether after recirculation STC water transfers further northward in the MOC. We find that 1.5 Sv of the water that recirculates in the northern STC at 2°N originates from interbasin exchange and will eventually transfer northward into the MOC. This implies that almost the entire northern STC consists of MOC water. For the southern STC this number is 2 Sv at 2°S while the total STC is 4 Sv. So half of the water masses recirculating in the southern STC are also part of the MOC. It appears that all the MOC water that takes a loop in the southern STC first crosses the equator

northward before it upwells. These parcels retroflect and come back to the equator where they upwell and transfer southward in the mixed layer in the Southern Hemisphere. As some MOC particles recirculate in both the northern and southern STC, we find that 2.7 Sv of MOC water recirculates in both STCs, that is 0.8 Sv of the water that recirculated in the southern STC also recirculates in the northern STC.

[24] Figure 9 summarizes the results for the different branches of the MOC and the STC in the Atlantic. There is 16 Sv of MOC inflow into the subtropical South Atlantic. Here 4.5 Sv becomes denser, due to drift in the model, and 6 Sv of MOC water does not upwell in the tropics and does not interact with the STCs. The remaining 5.5 Sv upwells in the mixed layer in the tropics. Here 2 Sv of the upwelled MOC water recirculates in the southern STC. Less than half of that transport (0.8 Sv) also recirculates in the northern
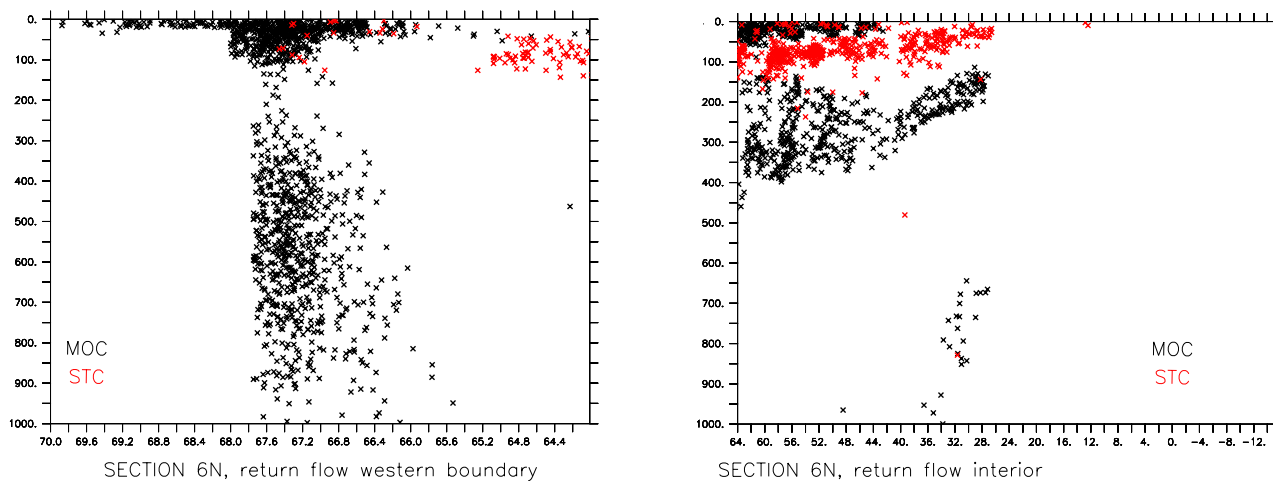


**Figure 7.** Cross section at 6°N of particles that were released at 2°N and traced forward until 6°N. This is the position where the particles pass 6°N for the last time. STC and MOC particles are distinguished, that is, MOC particles go northward at 20°N in the Atlantic basin and STC particles, when traced forward, return to 2°N below the mixed layer. Every 20th particle is shown.
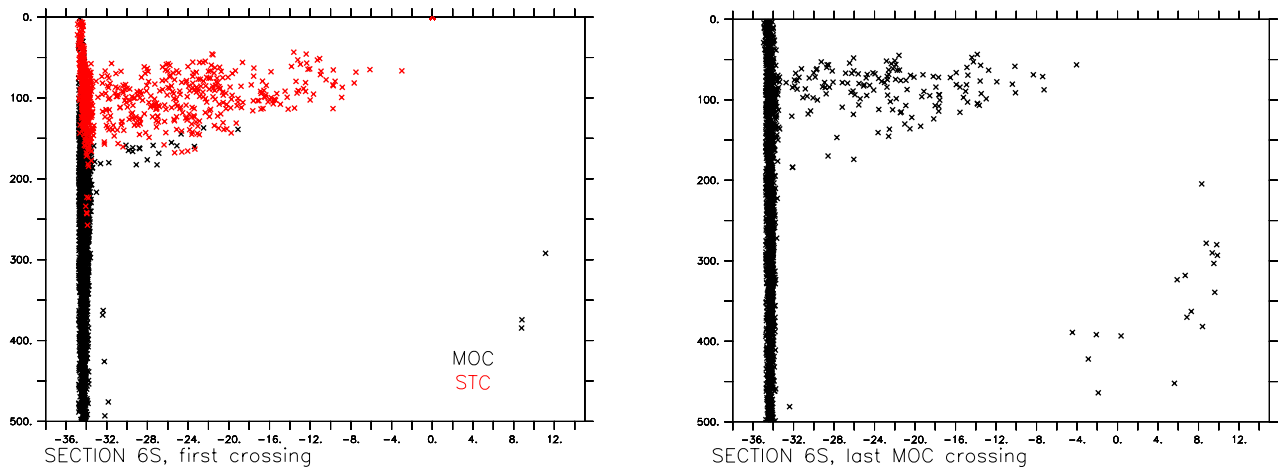
**Figure 8.** Cross section at 6°S of particles that were released at 2°S and traced backward until they cross 6°S for the first time (left). STC and MOC particles are distinguished as in previous figures. Cross section at 6°S of particles that were released at 10°S and traced forward until they cross 6°S for the last time before reaching 20°N (right).

STC, while 0.7 Sv recirculates exclusively in the northern STC. The remaining 2.8 Sv MOC water upwells into the mixed layer and does not recirculate in the STCs but transfers directly northward in the mixed layer only. After the total of 2.7 Sv has recirculated in the STCs it goes northward in the upper subtropical North Atlantic and joins the directly upwelled water. In the southern STC there is an additional 2 Sv recirculation of STC water that does not
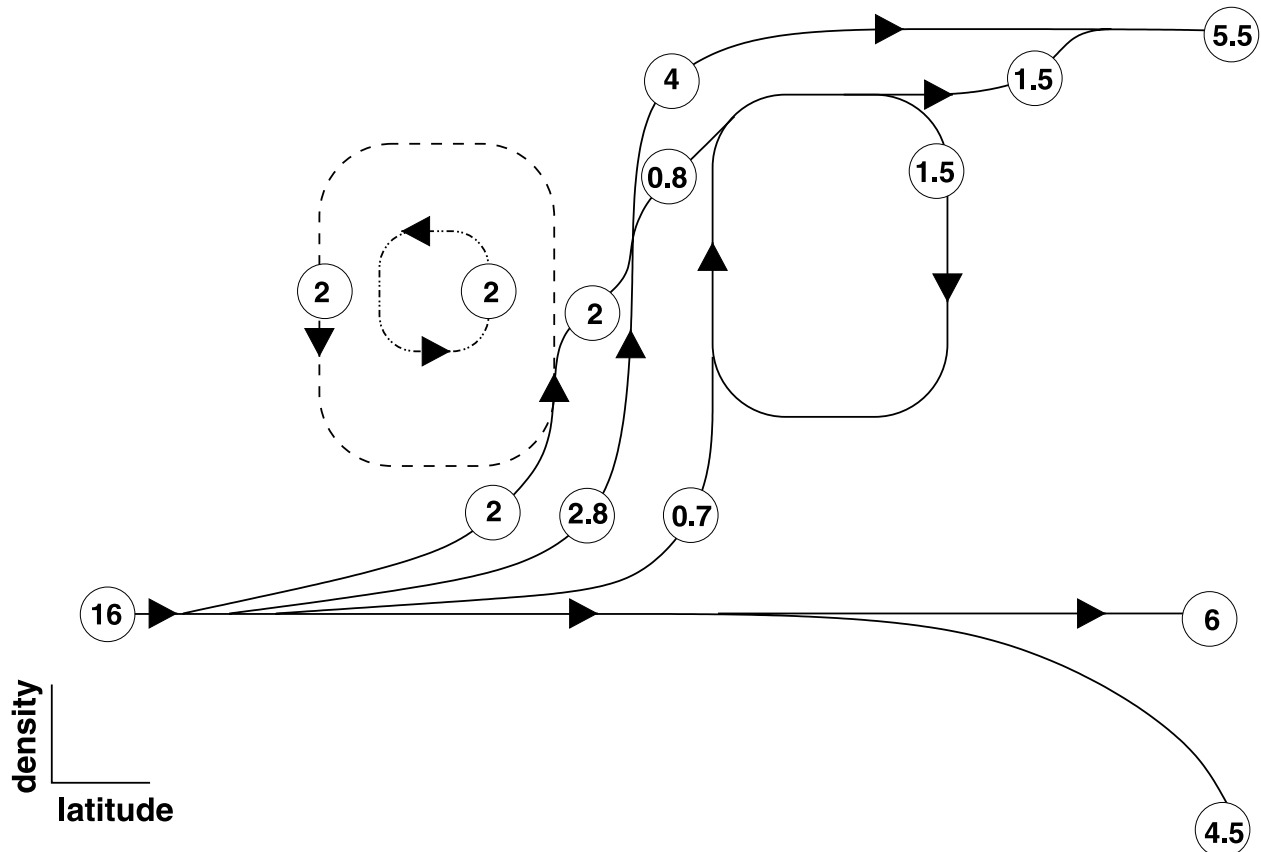


**Figure 9.** Schematic summarizing the results from the trajectory analysis of MOC and STC water masses in a latitude-density plane. 16 Sv of MOC water enters the South Atlantic on the left hand side of the schematic and its different branches are shown (numbers are transports in Sverdrups). The dashed lines indicate anticlockwise motion, continuous lines indicate clockwise motion. The dashed-dotted line shows recirculation of the southern STC only.
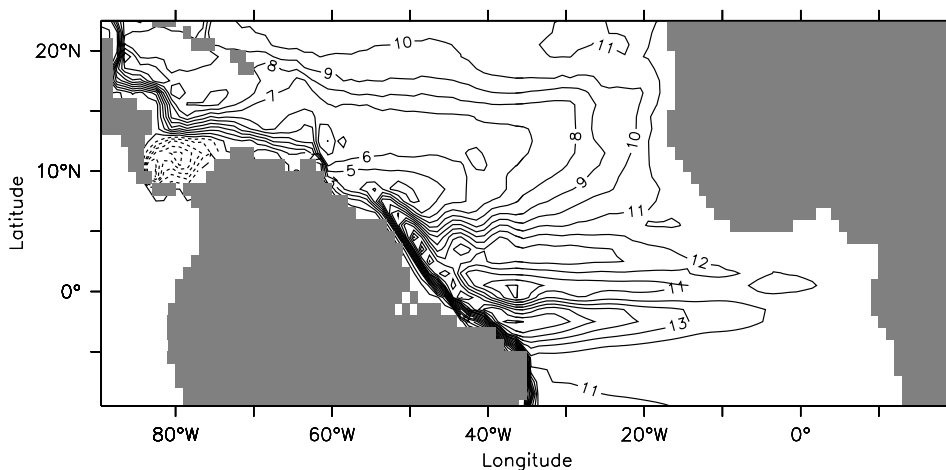
**Figure 10.** Stream function of particles that start at 10°S and leave at 20°N, that is, the upper limb of the MOC in the model (in Sv).

originate from the MOC resulting in a total STC strength of 4 Sv.

## 3.2. MOC Pathways in the Tropical Atlantic

[25] The water mass crossroads summarized in Figure 9 suggest an active role of the tropical Atlantic circulation in modifying MOC water masses. In this section we show the recirculation of MOC water masses in the tropical Atlantic in more detail. Figure 10 shows the Lagrangian stream function of particles that were released at 10°S and cross 25°N with a northward velocity. In contrast to the stream function shown in Figure 2, we see the recirculation of the water masses in the tropical gyres with large zonal excursions near the equator.

[26] The recirculation of MOC water masses in the equatorial current system becomes more apparent when we consider cross sections at 35°W and at 23°W (Figures 11 and 12). In Figure 12a we show the position of parcels that cross 35°W for the first time eastward. The Equatorial Undercurrent (EUC) stands out when the location of the particles is compared with the cross sections of zonal velocity (Figures 11a and 11d). The EUC carries 6.5 Sv of MOC water. About 0.8 Sv MOC water is carried in the North Equatorial Undercurrent at 3°N between 150 and 350 m of depth. Further east at 23°W the Equatorial Undercurrent still stands out (Figure 12c) and on both sides of it eastward transport is seen in the South Equatorial Undercurrent and in the North Equatorial Countercurrent. Only a small amount (0.4 Sv) is carried
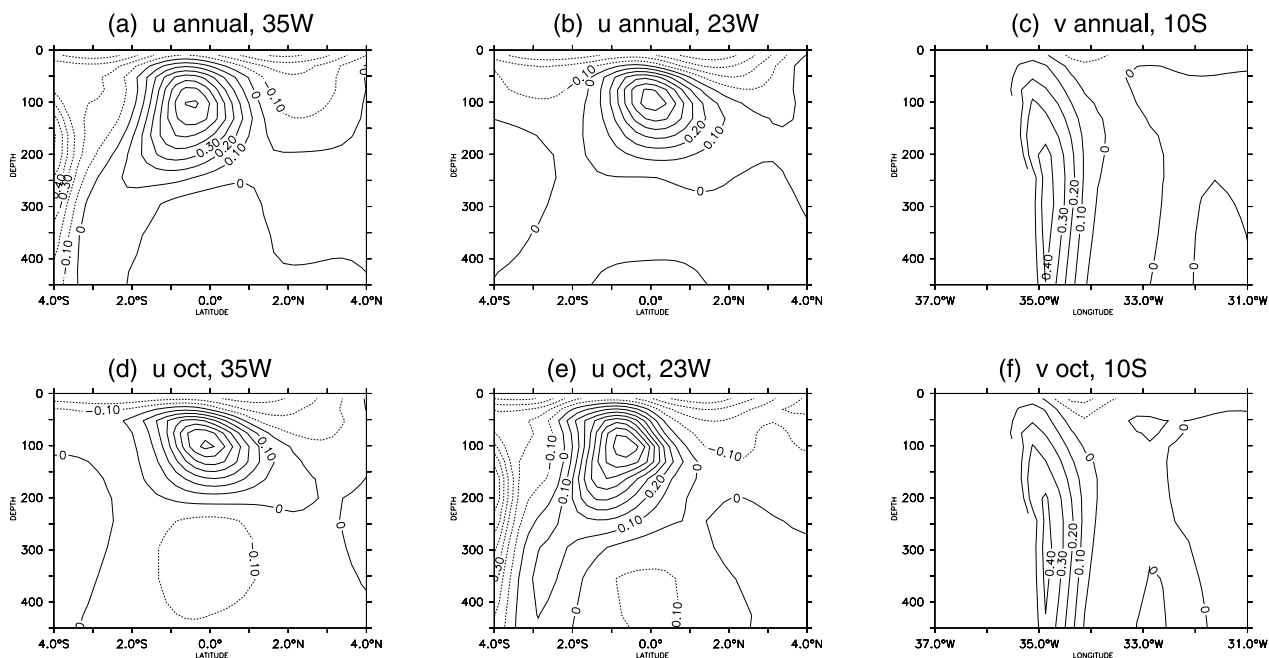


**Figure 11.** Cross sections of zonal velocities at 35°W and 23°W and meridional velocities at 10°S (in m s$^{-1}$). (a, b, c) Annual mean values. (c, d, e) October values.
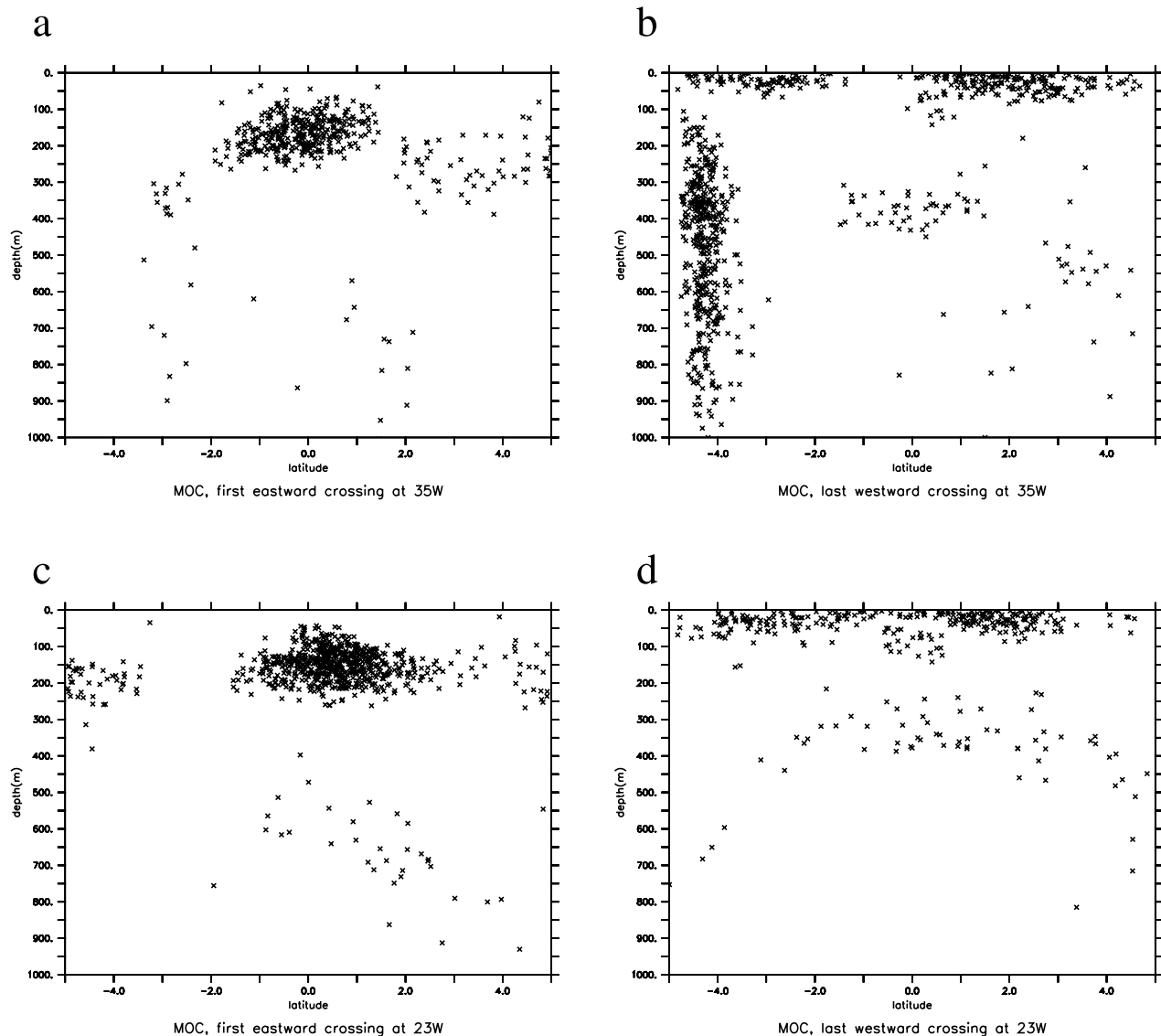
**Figure 12.** Cross sections at 35°W and at 23°W of particles that were released at 30°S and traced forward and leave the domain northward at 20°N. (a) Particles that pass 35°W for the first time eastward after release. (b) Particles that pass 35°W for the last time westward before leaving the domain. (c) Particles that pass 23°W for the first time eastward after release. (d) Particles that pass 23°W for the last time westward before leaving the domain (every 20th particle is shown). This figure shows the positions of MOC particles in the equatorial currents.

eastward by currents below 300 m. When we consider the positions of the westward propagating particles that pass 23°W for the last time we see that most MOC water has upwelled (Figure 12d). The branches of the South Equatorial Current stand out and transfer 5.5 Sv of upwelled MOC water westward.

[27] Below 300 m a total of 1 Sv is carried by intermediate currents and subsurface branch of the South Equatorial Current. These currents are not apparent in annual mean velocities (Figures 11a, 11b, and 11c), but the cross sections in October (Figures 11d, 11e, and 11f) show that these currents are present in autumn and can transfer MOC water masses. Finally, at 35°W we see the same picture as at 23°W, but now the North Brazil Undercurrent is visible

at the western boundary (Figure 12b and Figures 11c and 11f).

## 4. Discussion

### 4.1. Large-Scale Consequences

[28] We showed that about a third of the MOC water upwells in the tropics. A substantial amount of that water recirculates in the STCs. Upwelling of MOC water masses in the tropical Atlantic implies that its properties can change which may affect the stability of the MOC. The transformation of MOC water masses is clear from the temperature and salinity of MOC parcels when they enter the tropical Atlantic at 10°S compared to when they leave the region at
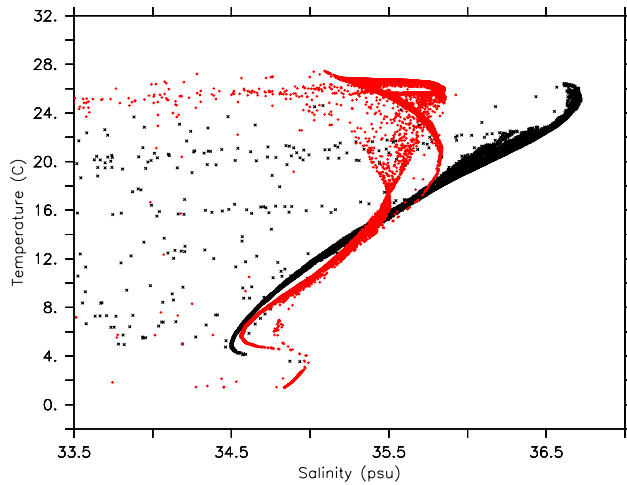
**Figure 13.** Temperature-salinity diagrams of MOC water that passes 10°S for the first time (black, shown by crosses) and that passes 10°N for the last time (grey, shown by pluses).

10°N (Figure 13). At 10°S, South Atlantic Central Water is found that is characterized by a linear temperature-salinity relationship [e.g., *Poole and Tomczak*, 1999]. The freshening of surface waters induced by the runoff and the Intertropical Convergence Zone is eminent. Also, the MOC water masses warm substantially. These results are consistent with the progressive warming and freshening toward the north found by *Stramma and England* [1999] in observations. The warming stands out when the volume transport of the MOC is binned in temperature and salinity classes (Figure 14). The redistribution of MOC waters is very clear as indicated by the large peak of volume transport at a temperature of about 26 degrees C at 10°N at the expense of volume transport in a range between 6 and 22 degrees C (Figure 14a). The slight cooling at low temperatures is also visible in the temperature salinity diagram and reflects the drift of intermediate water masses toward North Atlantic Deep Water that should be considered as unrealistic. Both freshening and salinifying of MOC water is found (Figure 14b). As can be seen from the Figure 13, the water masses at higher densities become more salty while the warmer surface waters freshen due to runoff and precipitation.

[29] To put these changes into perspective of the global ocean circulation, the heat uptake of MOC water masses in the tropical Atlantic is compared to estimates of divergences of meridional heat transport from observations in the Atlantic basin. We determine the amount of heat carried by the upper branch of the MOC from the thermodynamic properties of the trajectories at the sections at 10°N and 10°S according to

$$H_{moc} = \rho c_p \sum_i^N V_i T_i. \qquad (1)$$

Here $H_{moc}$ is the heat transport by the upper branch of the MOC, $V_i$ is the volume transport carried by each particle in the upper branch of the MOC, $T_i$ is the temperature of each

particle, $\rho$ is density of sea water, $c_p$ is the heat capacity, and $N$ is the number of particles that crosses a section. The heat transport by particles that make up the upper branch of the MOC is 0.86 PW (= $10^{15}$W) at 10°N. The change of heat that is carried northward by these particles between 10°S and 10°N, that is, the heat transport divergence is 0.22 PW. The observed total heat transport divergence in the tropical Atlantic Ocean between 10°N and 10°S is 0.43 PW based on *Da Silva et al.* [1994]. Using estimates from NCEP reanalysis data [*Trenberth and Caron*, 2001], we obtain a heat transport divergence of 0.49 PW. From ECMWF data we obtain a divergence of 0.42 PW.

[30] Similar to the heat transport through a section, the fresh water transport can be estimated from

$$F_{moc} = \frac{1}{S_0} \sum_i^N V_i S_i. \qquad (2)$$

Here, $F_{moc}$ is the fresh water transport by the upper branch of the MOC, $S_0$ is a reference salinity that has been set to 35 psu, and $S_i$ is the salinity of each particle that crosses a section. The fresh water transport divergence of MOC water masses between 10°N and 10°S is 0.16 Sv. The fresh water transports obtained from indirect and direct measurements vary strongly. Especially over regions of large precipitation, large variations are found. *Wijffels* [2001] summarizes different estimates and the total fresh water divergence is found between 0.2 and 0.4 Sv.

[31] The results from the trajectory analysis indicate that the tropics is indeed active in modifying MOC properties substantially. We conclude that in the tropical Atlantic at least half of the heat received from the atmosphere is used to heat up MOC water masses which transfer the heat northward in the ocean. The freshening of MOC water masses is also about half of the total fresh water transport divergence in the tropical Atlantic region.

### 4.2. Comparison to Observations

[32] The results shown in this paper are obtained with a numerical ocean model. Most ocean currents that are important for the MOC and STC circulations in the tropical Atlantic are well represented in this model. From the south the tropical Atlantic is fed by the South Equatorial Current and the North Brazil Undercurrent in accordance with, for instance, *Schott et al.* [1998] and *Stramma and England* [1999] (see Figures 1, 2, 3, and 11). In the equatorial region, the Equatorial Undercurrent is well represented [see also *Hazeleger et al.*, 2003] as well as the equatorial branches of the South Equatorial Current and the North Equatorial Counter Current. However, compared to observed transports presented by *Schott et al.* [2003] and *Stramma et al.* [2005], the model has too weak off-equatorial undercurrents. Also, *Schott et al.* [2003] report a permanently present Equatorial Intermediate Current beneath the Equatorial Undercurrent which we only find in autumn (Figure 11).

[33] The water mass analysis shown in Figures 13 and 14 shows that the main water masses are well represented by the model. In particular, South Atlantic Central Water is well represented as indicated by the linear temperature-salinity relationship [*Poole and Tomczak*, 1999]. These water mass characteristics compare well to the origin of

a

b
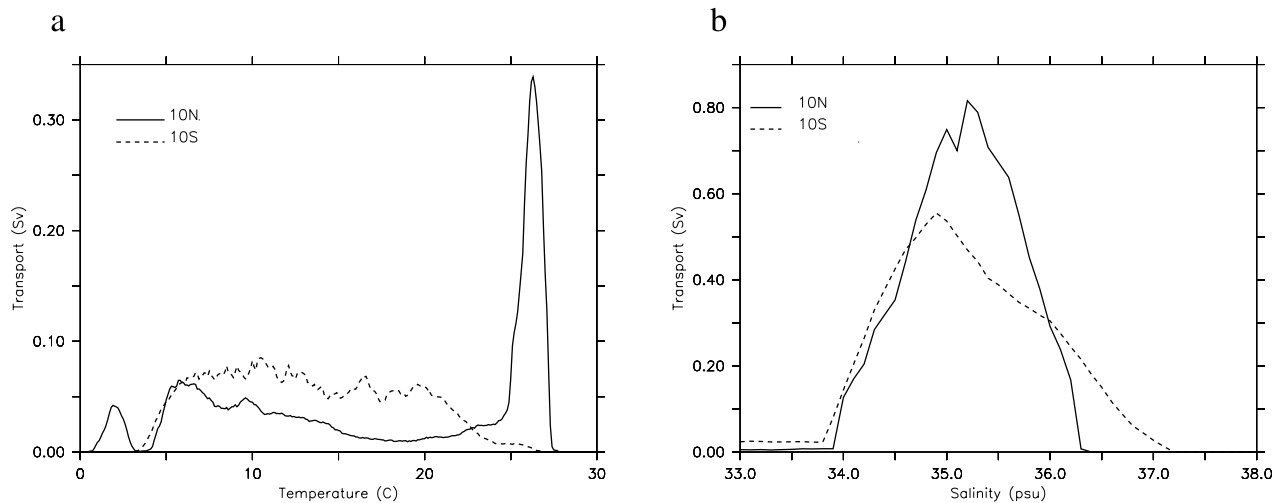


**Figure 14.** MOC volume transport binned in (a) temperature classes (bins of 0.1 C, smoothed with a 10-point box filter) and (b) salinity classes (bins of 0.1 psu, smoothed with a 10-point box filter) at sections at 10°S and 10°N.

Equatorial Undercurrent water presented by *Snowden and Molinari* [2003] and the observations presented by *Stramma and England* [1999]. In the following we will discuss in more detail comparisons between observed and modeled transports that are relevant to the MOC and STC circulations.

[34] The observed cross-equatorial exchange associated with the basin-wide meridional overturning circulation is on the order of 13 to 17 Sv [*Schmitz and Richardson*, 1991; *Schmitz 1995*; *Smethie and Fine*, 2001]. In the upper tropical Atlantic this consists of northward transport of warm surface water in primarily the North Brazil Current as part of the thermohaline overturning cell [*Gordon*, 1986]. The model analyzed here shows a realistic amount of 16 Sv of warm water inflow into the Atlantic originating from the Indian Ocean (Figure 2). This warm water is brought northward by the southern branch of the South Equatorial current and from 15°S on along the western boundary in the North Brazil Undercurrent. In addition, the tropical Atlantic is fed with 8 Sv of light surface water ($\sigma_\theta < 24.5$) from the central South Equatorial Current that entrains into the western boundary current at about 4°S as shown by *Schott et al.* [1998]. We see consistent amounts of transport when we add the STC and gyre flows at 4°S in the model (Figures 1 and 3).

[35] It is clear from our cross sections that the MOC waters stay along the western boundary on the Southern Hemisphere in the North Brazil Undercurrent. Although Figure 10 and 12 show that the MOC recirculates into the Equatorial Undercurrent, the Southern Equatorial Undercurrent, and Northern Equatorial Undercurrent, most of it remains at the western boundary while crossing the equator. Compared to an earlier model study by *Blanke et al.* [1999], we find more recirculation, with separate recirculation cells north and south of the equator.

[36] On the basis of water mass analysis and the number of North Brazil current rings shed per year, *Johns et al.* [2003] estimated that 9 Sv of South Atlantic water is transferred northward in rings along the western boundary. We find lower values (about 5 Sv, see Figure 2 and 10) and

get a more dominant pathway in the interior. This also implies a more prominent role of the cyclonic circulation centered near 12°N and 25°W (the Guinea Dome) in which MOC water can upwell and then expel northward in the mixed layer and transfer westward in the North Equatorial Current. However, it is possible that the model underestimates the ring transport because the horizontal resolution is eddy-permitting. Alternatively, the pathways can be sensitive to the atmospheric forcing that is used to force the ocean [*Inui et al.*, 2002]

[37] One of the purposes of this study is to disentangle the MOC transports from the STC transports and to study how much the STC and MOC interact. *Zhang et al.* [2003] use western boundary current transport, interior transport, and upwelling transport to infer STC and MOC transports from observations. The values they find are upper limits of STC-MOC interaction.

[38] *Zhang et al.* [2003] find equatorward flow of 2 Sv in the Northern Hemisphere in the interior, just as we do. At 6°S they find 4 Sv of equatorward transport in the interior which they interpret as STC transport. We find only 2 Sv equatorward transport in the STC at this latitude. However, Zhang et al. determine this equatorward transport using hydrographic data and this does not imply that the equatorward flow actually upwells. We find a similar number if we add the STC transport and the interior gyre flow.

[39] At the western boundary a 3 Sv equatorward flow on the Northern Hemisphere is assumed based on a sparse data set by *Bourles et al.* [1999]. We do not find equatorward STC transport along the western boundary, but the return flow between 65°W and 25°W seen at 6°N (Figure 7) may be interpreted as the southeastward Guiana Undercurrent and a southward branch of the North Equatorial Current of the model. In the Southern Hemisphere the western boundary current transports used by *Zhang et al.* [2003] and those that are found here are similar: 12 Sv.

[40] The total upwelling found by *Zhang et al.* [2003] is 21 Sv based on divergences from drifter data. We find a similar upwelling from Eulerian mean transports, but the Lagrangian mean upwelling is less, as some upwelling

occurs within the mixed layer and is compensated by eddies [see *Hazeleger et al.*, 2003; *Hazeleger and de Vries*, 2003]. The net obduction is only 7.5 Sv (5.5 from the MOC and 2 Sv from the southern STC). The 5.5 Sv upwelling of MOC waters is consistent with *Roemmich* [1983], who found 6 Sv of MOC upwelling from observations. We find that 2.7 Sv of the 5.5 Sv recirculates in the STCs. This recirculation has not been taken into account by Zhang et al. The much higher upwelling rates and the different Northern Hemisphere western boundary current transport used by Zhang et al. imply much stronger STCs in their study. We argue that a substantial amount of the upwelling is associated with tropical cells which are largely compensated by eddy transports.

[41] It is hard to judge whether the observational data was too sparse or whether the model contains errors. The advantage of the model is that the upwelled water and the gyre flow could be separated unambiguously, as well as the interaction between the MOC and the STC. *Zhang et al.* [2003] did not take this recirculation into account explicitly and had to close their budget with the relatively uncertain western boundary transports and the surface layer divergence obtained from drifter data. It is clear that this is a daunting task using the observations. However, model uncertainties can be the cause of these discrepancies as well. As stated before, the ventilation of the tropical thermocline depends on the wind product that is used. Also, the strength of the vertical mixing relates to the strength of STCs [*Boccaletti et al.*, 2004] and the Eulerian mean transport through the base of the mixed layer differs from the upwelling with eddy-induced transports included. Here, we did include the eddy-induced transports that are hard to obtain from observations.

## 5. Summary and Conclusions

[42] The zonally averaged circulation in the tropical Atlantic is dominated by the wind-driven STCs and thermohaline driven basin-wide MOC. Here, we presented a Lagrangian analysis of the three-dimensional spatial patterns of these circulations in a high-resolution ocean model. The analysis enabled us to separate the shallow wind-driven overturning from the basin-wide overturning. On first approach from the south toward the equator the STC and the MOC are clearly separated. Here 16 Sv of MOC water approaches the equator along the South Equatorial Current and the the North Brazil Current, while 4 Sv of STC water recirculates in the Southern Hemisphere. The MOC is located at deeper depths than the STC but both are confined primarily to the western boundary current region. Here 6 Sv of MOC water enters the Equatorial Undercurrent and a total of 5.5 Sv of MOC water finally upwells in the mixed layer and can be transformed by surface fluxes. After upwelling at the equator, 2 Sv of MOC water recirculates in the southern STC, showing that both overturning cells interact. After crossing the equator, about half of the MOC water transfers northward along the western boundary. The other half turns eastward in the North Equatorial Countercurrent and loops cyclonically northward and joins the westward North Equatorial Current. The STC on the Northern Hemisphere has a strength of only 1.5 Sv and is confined to the retroflection area close to the western

boundary. Almost all water that it transfers is part of the MOC. That is, most of the northward flow in the upper layer and the southward return flow eventually transfers northward to higher latitudes. In total, 2.7 Sv of the 5.5 Sv of MOC water that upwells in the tropical Atlantic recirculates in the STCs (Figure 9 summarizes these MOC and STC branches). These results imply that MOC properties alter by surface fluxes in the tropics, but it also implies that anomalies in the MOC can impact the STC and possibly tropical Atlantic climate associated with tropical upwelling. Substantial warming and freshening is found. 0.22 PW is taken up from the atmosphere to warm up MOC water masses in the tropical Atlantic, which is about half of the total heat exchange between ocean and atmosphere in this region. 0.16 Sv fresh water transport divergence is found.

[43] Many features of the STC and MOC pathways in the model compare well with observed estimates of, for instance, *Schott et al.* [1998] and *Zhang et al.* [2003]. Especially interior transports and western boundary transports in the south compare well. However, owing to uncertainties in the upwelling and in the western boundary transports in the north discrepancies are found. This prompts for further research and need for more data of upwelling rates and western boundary current transports.

## References

Blanke, B., and S. Raynaud (1997), Kinematics of the Pacific equatorial undercurrent: An Eulerian and Lagrangian approach from GCM results, *J. Phys. Oceanogr.*, *27*, 1038–1053.

Blanke, B., M. Arhan, G. Madec, and S. Roche (1999), Warm water paths in the Equatorial Atlantic as diagnosed with a general circulation model, *J. Phys. Oceanogr.*, *29*, 2753–2768.

Boccaletti, G., R. C. Pacanowksi, S. G. H. Philander, and A. V. Federov (2004), The thermal structure of the upper ocean, *J. Phys. Oceanogr.*, *34*, 888–902.

Bourles, B., R. L. Molinari, W. E. Johns, W. D. Wilson, and K. D. Leaman (1999), Upper layer currents in the western tropical North Atlantic (1989–1991), *J. Geophys. Res.*, *104*, 1361–1375.

Da Silva, A. M., C. C. Young, and S. Levitus (1994), *Algorithms and Procedures*, vol. 1, *Atlas of Surface Marine Data 1994*, NESDIS 6, 83 pp., NOAA, Washington, D. C.

de Vries, P., and K. Döös (2001), Calculating Lagrangian trajectories using time-dependent velocity fields, *J. Atmos. Oceanic Technol.*, *18*, 1092–1101.

Donners, J., S. S. Drijfhout, and W. Hazeleger (2005), Water mass transformation and subduction in the South Atlantic, *J. Phys. Oceanogr.*, *35*, 1841–1860.

Döös, K. (1995), Interocean exchange of water masses, *J. Geophys. Res.*, *100*, 13,499–13,514.

Drijfhout, S. S., P. de Vries, K. Döös, and A. C. Coward (2003), Impact of eddy-induced transport on the Lagrangian structure of the upper branch of the thermohaline circulation, *J. Phys. Oceanogr.*, *33*, 2141–2155.

Fratantoni, D. M., W. E. Johns, T. L. Townsend, and H. E. Hulburt (2000), Low-latitude circulation and mass transport pathways in a model of the tropical Atlantic ocean, *J. Phys. Oceanogr.*, *30*, 1944–1966.

Gibson, R., P. Kallberg, S. Uppala, A. Hernandez, A. Nomura, and E. Serrano (1997), The ERA description, in *The ECMWF Re-Analysis Proj. Rep. Ser. 1*, ECMWF, Reading, UK.

Goodman, P. J., W. Hazeleger, P. de Vries, and M. Cane (2005), Pathways into the Pacific Equatorial Undercurrent: A trajectory analysis, *J. Phys. Oceanogr.*, *35*, 2134–2151.

Gordon, A. L. (1986), Interocean exchange of thermocline water, *J. Geophys. Res.*, *91*, 5037–5046.

Halliwell, G. R., R. H. Weisberg, and D. A. Mayer (2003), A synthetic float analysis of upper limb meridional overturning circulation interior pathways ocean pathways in the tropical/subtropical Atlantic, in

*Interhemispheric Water Exchange in the Atlantic Ocean*, Elsevier Oceanogr. Ser., vol. 68, edited by G. J. Goni and P. Malanotte-Rizzoli, pp. 93–136, Elsevier, New York.

Hazeleger, W., and P. de Vries (2003), Fate of the Equatorial Undercurrent in the Atlantic, in *Interhemispheric Water Exchange in the Atlantic Ocean*, Elsevier Oceanogr. Ser., vol. 68, edited by G. J. Goni and P. Malanotte-Rizzoli, pp. 175–191, Elsevier, New York.

Hazeleger, W., P. de Vries, and Y. Friocourt (2003), Sources of the Equatorial Undercurrent in the Atlantic in a high-resolution ocean model, *J. Phys. Oceanogr.*, 33, 677–693.

Inui, T., A. Lazar, P. Malanotte-Rizzoli, and A. Busalacchi (2002), Wind stress effects on the Atlantic Subtropical-Tropical circulation, *J. Phys. Oceanogr.*, 32, 2257–2276.

Jochum, M., and P. Malanotte-Rizzoli (2001), Influence of the meridional overturning circulation on tropical-subtropical pathways, *J. Phys. Oceanogr.*, 31, 1313–1323.

Johns, W. E., T. N. Lee, F. A. Schott, R. J. Zantopp, and R. H. Evans (1990), The North Brazil Current retroflection: Seasonal structure and eddy variability, *J. Geophys. Res.*, 95, 22,103–22,120.

Johns, W. E., R. Zantopp, and G. Goni (2003), Cross-gyre transport by North Brazil Current rings, in *Interhemispheric Water Exchange in the Atlantic Ocean*, Elsevier Oceanogr. Ser., vol. 68, edited by G. J. Goni and P. Malanotte-Rizzoli, pp. 411–442, Elsevier, New York.

Killworth, P. D. (1996), Time interpolation of forcing fields in ocean models, *J. Phys. Oceanogr.*, 26, 136–143.

Levitus, S., and T. Boyer (1994), *World Ocean Atlas 1994*, vol. 4, *Temperature: NOAA Atlas NESDIS 4*, 117 pp., NOAA, Washington, D.C.

Levitus, S., R. Burgett, and T. Boyer (1994), *World Ocean Atlas 1994*, vol. 3, *Salinity: NOAA Atlas NESDIS 3*, 99 pp., NOAA, Washington, D.C.

Malanotte-Rizzoli, P., K. Hedstrom, H. Arango, and D. B. Haidvogel (2000), Water mass pathways between the subtropical and tropical ocean in a climatological simulation of the North Atlantic ocean circulation, *Dyn. Atmos. Oceans*, 32, 331–371.

McCreary, J. P., and P. Lu (1994), On the interaction between the subtropical and equatorial ocean circulation: The subtropical cell, *J. Phys. Oceanogr.*, 24, 466–497.

Pacanowski, R. C., and S. G. H. Philander (1981), Parameterization of vertical mixing in numerical models of tropical oceans, *J. Phys. Oceanogr.*, 11, 1051–1443.

Poole, R., and M. Tomczak (1999), Optimum multiparameter analysis of the water mass structure in the Atlantic Ocean thermocline, *Deep Sea Res.*, 46, 1895–1921.

Reynolds, R. W., and T. M. Smith (1994), Improved global sea surface temperature analyses, *J. Clim.*, 7, 929–948.

Roemmich, D. (1983), The balance of geostrophic and Ekman transport in the tropical Atlantic Ocean, *J. Phys. Oceanogr.*, 13, 1534–1539.

Schmitz, W. J. (1995), On the interbasin-scale thermohaline circulation, *Rev. Geophys.*, 33, 151–173.

Schmitz, W. J., and P. L. Richardson (1991), On the sources of the Florida Current, *Deep Sea Res.*, 38, suppl. 1, 5379–5409.

Schott, F. A., J. Fischer, and L. Stramma (1998), Transports and pathways of the upper-layer circulation in the western tropical Atlantic, *J. Phys. Oceanogr.*, 28, 1904–1918.

Schott, F. A., M. Dengler, P. Brandt, K. Affler, J. Fischer, B. Bourles, Y. Gouriou, R. L. Molinari, and M. Rhein (2003), The zonal currents and transports at 35°W in the tropical Atlantic, *Geophys. Res. Lett.*, 30(X), 1349, doi:10.1029/2002GL016849.

Smethie, W. M., and R. A. Fine (2001), Rates of North Atlantic deep water formation calculated from chlorofluorocarbon inventories, *Deep Sea Res.*, 48, 189–215.

Snowden, D. P., and R. L. Molinari (2003), Subtropical cells in the Atlantic Ocean: An observational summary, in *Interhemispheric Water Exchange in the Atlantic Ocean*, Elsevier Oceanogr. Ser., vol. 68, edited by G. J. Goni and P. Malanotte-Rizzoli, pp. 287–312, Elsevier, New York.

Stramma, L., and M. England (1999), On the water masses and mean circulation of the South Atlantic Ocean, *J. Geoph. Res.*, 104, 20,863–20,883.

Stramma, L., M. Rhein, P. Brandt, M. Dengler, C. Böning, and M. Walter (2005), Upper layer ocean circulation in the western tropical Atlantic boreal fall 2000, *Deep Sea Res. I*, 52, 221–240.

Trenberth, K. E., and J. M. Caron (2001), Estimates of meridional atmosphere and ocean heat transports, *J. Climate*, 14, 3433–3443.

Webb, D. J., A. C. Coward, B. A. de Cuevas, and C. S. Williams (1997), A multiprocessor ocean general circulation model using message passing, *J. Atmos. Oceanic Technol.*, 14, 175–183.

Wijffels, S. E. (2001), Ocean transport of fresh water, in *Ocean Circulation and Climate*, Int. Geophys. Ser., vol. 77, edited by G. Siedler, J. Church, and J. Gould, pp. 475–488, Elsevier, New York.

Zebiak, S. E. (1993), Air-sea interaction in the equatorial Atlantic region, *J. Clim.*, 6, 1567–1586.

Zhang, D., M. J. McPhaden, and W. E. Johns (2003), Observational evidence for flow between the subtropical and tropical Atlantic: The Atlantic Subtropical Cells, *J. Phys. Oceanogr.*, 33, 1783–1797.

———————————

S. Drijfhout and W. Hazeleger, Oceanographic Research, Royal Netherlands Meteorological Institute, P. O. Box 201, 3730 AE, de Bilt, Netherlands. (wilco.hazeleger@knmi.nl)